


V. KOCHERGIN¹,
M. CHRISTOPHERSEN¹
H. FÖLL²

Surface plasmon enhancement of an optical anisotropy in porous silicon/metal composite

¹ Lake Shore Cryotronics, Inc., Columbus, OH 43082, USA

² Materials Science, Faculty of Engineering, University of Kiel, Kaiserstr. 2, 24143 Kiel, Germany

Received: 26 June 2004/Revised version: 14 September 2004

Published online: 26 October 2004 • © Springer-Verlag 2004

ABSTRACT We report on the theoretical results obtained by applying the modified effective medium theory to a composite material consisting of mesoporous Si on (110)-oriented substrate with pores filled with silver through, e.g., electroplating process. The theory developed permits a self-consistent determination of the effective dielectric permittivity tensor of such materials. It is shown that the optical anisotropy of such a composite can be greatly enhanced at some wavelength ranges. While this anisotropy is generally uniaxial as in non-metal-filled mesoporous Si etched on (110) substrate, the “sign” of the anisotropy (i.e., positive or negative) changes in some portions of the spectrum. The optimum material parameters for an experimental observation of the theoretically predicted effects are determined.

PACS 78.20.-e; 78.20.Bh; 78.20.Ci; 78.20.Fm; 78.30.Fs; 78.55.Mb

1 Introduction

Porous semiconductor materials (see, for example, [1] and references therein) offer the potentially important capability of engineering many optical properties at will. Semiconductors are usually turned porous by electrochemical (or photoelectrochemical) etching of the nonporous semiconductor substrates in some suitable electrolytes. To date, it has been shown that many types of semiconductors can be porous by these methods. The most popular example is porous silicon, which allows tailoring the pore geometry from micropores (pore diameters below 2 nm; often referred to as “nanopores”), via mesopores (pore diameters between 2–50 nm) to macropores (pore diameters above 50 nm). The usefulness of such materials for various optical components was already outlined in [2–5]. Quite recently it has been shown [6–9] that mesoporous silicon obtained from a (110) oriented substrate exhibits in-plane uniaxial optical anisotropy. A remarkable result is that in the near infrared and infrared spectral ranges such a material offers larger values of optical birefringence than that of any commonly known natural material.

From another point of view, metal filling of the pore arrays through e.g., electroplating or electroless plating techniques has been already demonstrated (see, for example, [4, 10, 11]). Some of the metals, e.g., silver, gold, aluminum, copper, are known as a good providers of surface plasmons (SPs), with nonradiative waves existing on the metal-semiconductor interfaces. SPs are known to be responsible for large enhancements of the electromagnetic field and to influence or dominate the scattering cross-section of metal colloids [12], Raman scattering, higher harmonic generation [13], etc. The question arises on how the linear optical properties (e.g., anisotropy) of the porous semiconductor (such as for example mesoporous silicon etched on (110) substrate) will change if the pores will be filled with SP-active metals.

To answer this question, we present in this paper a method for calculating the effective dielectric constants and refractive indices of metal-filled porous materials. Previously [5–7], the Bruggeman method [14], generalized for the case of single sub-lattices of oblate ellipsoids, was used for calculations of the optical effects in these materials. Such a generalization of the Bruggeman method provided fair estimates for the case of mesoporous (110)-oriented Si with unfilled pores. However, this approach is not applicable for the structures analyzed here. The new method presented here has the capability to analyze anisotropic mesoporous silicon structures with SP-active metal-filled pores. It considers the porous semiconductor medium as macroscopically homogeneous and assigns a dielectric permittivity tensor.

2 Effective permittivity tensor calculations

In order to apply the model we first need to determine the structure of the mesoporous silicon layer grown on (110) substrate. As was shown in [15], pores in mesoporous Si propagate preferentially in equivalent $\langle 100 \rangle$ crystallographic directions independently of the substrate orientation. Hence, it can be represented as a mixture of three lattice subsets of pores collinear to the crystallographic directions mentioned. However, not all $\langle 100 \rangle$ directions are equivalent; $\langle 100 \rangle$ directions more in line with the electrical field are preferred. This is certainly due to the fact that the electric field strength at the tip then is enlarged, enabling avalanche breakdown [16] and enhancing the electrochemical dissolution reaction at the pore tip.

 Fax: +1-614-818-1607, E-mail: vkochergin@lakeshore.com

in [001]), the coordinate transformation matrices will be as follows:

$$\hat{A}^{(1)} = \begin{pmatrix} \frac{\sqrt{2}}{2} & 0 & -\frac{\sqrt{2}}{2} \\ 0 & 1 & 0 \\ \frac{\sqrt{2}}{2} & 0 & \frac{\sqrt{2}}{2} \end{pmatrix}, \quad \hat{A}^{(2)} = \begin{pmatrix} -\frac{\sqrt{2}}{2} & 0 & \frac{\sqrt{2}}{2} \\ 0 & -1 & 0 \\ \frac{\sqrt{2}}{2} & 0 & \frac{\sqrt{2}}{2} \end{pmatrix},$$

$$\hat{A}^{(3)} = \begin{pmatrix} 0 & 1 & 0 \\ -1 & 0 & 0 \\ 0 & 0 & 1 \end{pmatrix}.$$

If the porosity of the mesoporous silicon layer is p and the coefficient r will be introduced to describe the ratio of filling fractions between the [001] metal-filled pore lattice and the overall porosity of the sample, the electrical polarization matrices $M^{(i)}$ for each lattice will be as follows:

$$M^{(1)} = M^{(2)} = \begin{pmatrix} \frac{(p-pr)\alpha_{1,1}^{(i)}}{2\varepsilon_{\text{Si}} - L_{1,1}(p-pr)\alpha_{1,1}^{(i)}} & 0 & 0 \\ 0 & \frac{2(p-pr)\alpha_{2,2}^{(i)}}{\varepsilon_{\text{Si}} - (1-L_{1,1})(p-pr)\alpha_{2,2}^{(i)}} & 0 \\ 0 & 0 & \frac{2(p-pr)\alpha_{3,3}^{(i)}}{\varepsilon_{\text{Si}} - (1-L_{1,1})(p-pr)\alpha_{3,3}^{(i)}} \end{pmatrix}$$

$$M^{(3)} = \begin{pmatrix} \frac{pr\alpha_{1,1}^{(3)}}{\varepsilon_{\text{Si}} - L_{1,1}pr\alpha_{1,1}^{(3)}} & 0 & 0 \\ 0 & \frac{2pr\alpha_{2,2}^{(3)}}{2\varepsilon_{\text{Si}} - (1-L_{1,1})pr\alpha_{2,2}^{(3)}} & 0 \\ 0 & 0 & \frac{2pr\alpha_{3,3}^{(3)}}{2\varepsilon_{\text{Si}} - (1-L_{1,1})pr\alpha_{3,3}^{(3)}} \end{pmatrix}.$$

If the metal inclusions in different subsets have the same shape and volume but different orientations, as we assumed originally, we have $\alpha_{i,j}^{(k)} = \alpha_{i,j}^{(l)}$. To determine these coefficients $\alpha_{i,j}^{(k)}$ we will use the result of Kuwata [12] for calculations of the normalized (by volume) polarizabilities of metal ellipsoids, which states

$$\alpha_{i,i}(\varepsilon) = \frac{1}{(L_{i,i} + \frac{\varepsilon}{\varepsilon_m - \varepsilon}) + A_{i,i}\varepsilon_m x_i^2 + B_{i,i}\varepsilon_m^2 x_i^4 - i\frac{4}{3}\pi^2 \varepsilon_m^{2/3} \frac{V}{\lambda^3}} \quad (3)$$

where $x_1 = \pi \frac{a}{\lambda}$; $x_2 = x_3 = \pi \frac{b}{\lambda}$; $A_{i,i} = -0.4865L_{i,i} - 1.046L_{i,i}^2 + 0.8481L_{i,i}^3$, $B_{i,i} = 0.01909L_{i,i} + 0.1999L_{i,i}^2 + 0.6077L_{i,i}^3$; λ is the wavelength.

Formula (3), according to [12] is valid for metal inclusion dimensions with sides in the range from just a few nanometers to at least a hundred of nanometers.

The spectral dependences of the polarizability coefficients for the case of a silver elongated ellipsoid with $a = 15$ nm and $b = 10$ nm, embedded into a silicon host was calculated with (3); the results are given in Fig. 2.

The dielectric constant of silver was calculated according to the Drude approximation. For the calculations the imaginary part of the silicon refractive index at the given wavelengths was neglected. The reason for this is that in porous

silicon the position of the absorption edge is strongly blue-shifted (see [21]), so such an assumption indeed makes sense. As one can expect, the polarizability resonances of the silver ellipsoids for electric fields of the electromagnetic wave aligned along different ellipsoid axes are located at different wavelengths. These polarizability resonances are related to the excitation of the surface plasmon modes on the ellipsoid surface.

By substituting (3) into (1) and calculating the coefficients of dielectric permittivity tensor of silver-porous silicon etched on (110) substrate composite one can show that the resultant material will exhibit an uniaxial type of anisotropy with the optical axis coinciding with the (001) silicon crystallographic direction. The optical anisotropy of such a material is well known (see, for example, [22]). In such crystals, two eigen-solutions of the secular equation exist for any direction of the electric field of the electromagnetic wave, which are called ordinary and extraordinary waves, respectively, have different polarization states, and are described by refractive indices usually denoted n_o and n_e . In the coordinate system as drawn in Fig. 1, $n_o = \sqrt{\varepsilon_{xx}^{(\text{eff})}} \equiv \sqrt{\varepsilon_{zz}^{(\text{eff})}}$, while $n_e = \sqrt{\varepsilon_{yy}^{(\text{eff})}}$. The normal surface of the electromagnetic waves in this case consists of a sphere and an ellipsoid of revolution and a sphere. The ordinary wave with the refractive index n_o is polarized such that the electric field of the electromagnetic wave is in the (001) plane. The extraordinary wave has a refractive index defined by $\frac{1}{n_e^2(\theta)} = \frac{\cos^2\theta}{n_o^2} + \frac{\sin^2\theta}{n_e^2}$, where θ is the angle between the electromagnetic wave propagation direction and the [001] crystal axis, and its polarization for the case of the plane of incidence

being the (1 $\bar{1}$ 0) plane, is given by $\begin{pmatrix} 0 \\ \frac{\cos\theta}{n_e^2(\theta) - n_o^2} \\ \frac{\sin\theta}{n_e^2(\theta) - n_o^2} \end{pmatrix}$.

The numerically calculated spectral dependences of the real (n) and imaginary (k) parts of ordinary and extraordinary refractive indices of the material with filling fraction of the silver ellipsoids of just 0.1 volume percent

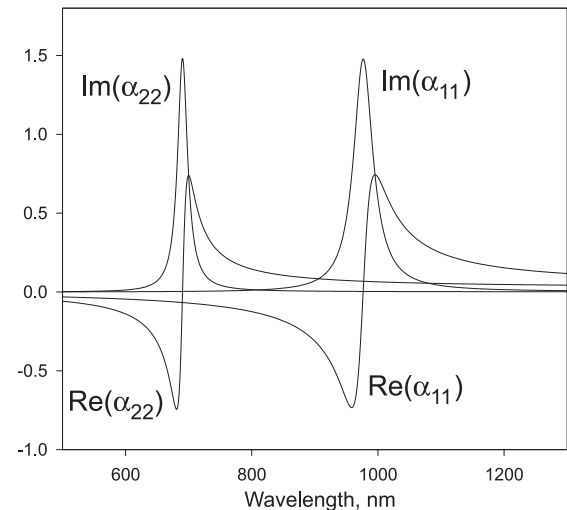


FIGURE 2 Numerically calculated spectral dependences of the polarizability tensor coefficients of the elongated silver ellipsoid with $a = 15$ nm and $b = 10$ nm, embedded into silicon host

are given in Fig. 3. One can see that the model predicts a substantial optical anisotropy of such a material, even for the small filling fractions used, and that the uniaxial anisotropy of the material changes the “sign” (from positive to negative) around the positions of the surface plasmon resonances.

It should be noted that the model presented above can provide reasonable results only for very small filling fractions of metal ellipsoids, especially around the resonances. Moreover, such a model can only predict the dielectric properties of composites consisting of weakly-polarizable inclusions fairly realistically; for such highly-polarizable inclusions as metal ellipsoids around plasmon resonance excitation conditions, the model is not really adequate. More self-consistent models need to be implemented and the rest of the paper is devoted to this task.

In this paper we use the generalization of the Bruggeman [14] method on the case of composite consisting of multiple sublattices of inclusions. The main assumption in the Bruggeman method is that the total electrical polarizability of the composite material is equal to zero. In other words, the total polarizability of all the inclusions (in our case both metal inclusions and silicon “inclusions”) embedded in the medium with effective dielectric parameters should vanish:

$$\sum_{i=1}^3 \tilde{P}^{(i)} + \tilde{P}^{(4)} = 0 \quad (4)$$

where $\tilde{P}^{(i)}$, $i = 1, 2, 3$ is the polarization of the i th lattice subset and $\tilde{P}^{(4)}$ is the polarizability of the Si “inclusion” in the matrix. According to the abbreviations introduced above, (4) can be rewritten in our case in the following form:

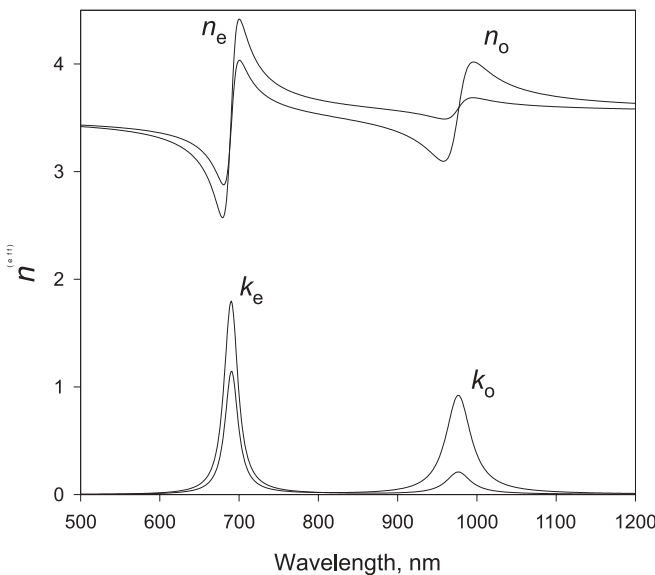


FIGURE 3 Numerically calculated spectral dependences of the real (n) and imaginary (k) parts of ordinary and extraordinary refractive indices of the silver/porous silicon etched on (110)-oriented wafer with filling fraction of the silver ellipsoids of 0.1 volume percent

$$(1-p)\hat{\alpha}^{(4)}\vec{E} + \frac{p-pr}{2}\hat{A}^{(1)}\hat{\alpha}^{(1)}\hat{A}^{(1)-1}\vec{E} + \frac{p-pr}{2}\hat{A}^{(2)}\hat{\alpha}^{(2)}\hat{A}^{(2)-1}\vec{E} + pr\hat{A}^{(3)}\hat{\alpha}^{(3)}\hat{A}^{(3)-1}\vec{E} = 0 \quad (5)$$

Generally, (5) states a fairly complex problem since it includes the determination of the polarizabilities of the all inclusions in the anisotropic medium with generally speaking unknown orientations of the axes, and thus requires solving a system of six independent equations with six unknowns (according to the number of independent coefficients in the dielectric permittivity tensor of the effective medium). However, in our case we can simplify the solution of problem (5) by using the results obtained by using the generalization of the Maxwell-Garnet model already introduced. Although, as mentioned before, this model cannot provide sufficiently accurate quantitative results for the material analyzed here, the qualitative predictions of an uniaxial type of anisotropy with optical axis aligned with the $\langle 001 \rangle$ crystallographic direction can certainly be trusted. Taking this into account, we can write the polarizability tensors of metal inclusions in each lattice subset as:

$$\hat{\alpha}^{(1)} = \begin{pmatrix} \alpha_{1,1}(\varepsilon_o) & 0 & 0 \\ 0 & \alpha_{2,2}(\varepsilon_e) & 0 \\ 0 & 0 & \alpha_{3,3}(\varepsilon_o) \end{pmatrix},$$

$$\hat{\alpha}^{(2)} = \begin{pmatrix} \alpha_{1,1}(\varepsilon_o) & 0 & 0 \\ 0 & \alpha_{2,2}(\varepsilon_e) & 0 \\ 0 & 0 & \alpha_{3,3}(\varepsilon_o) \end{pmatrix},$$

$$\hat{\alpha}^{(3)} = \begin{pmatrix} \alpha_{1,1}(\varepsilon_e) & 0 & 0 \\ 0 & \alpha_{2,2}(\varepsilon_o) & 0 \\ 0 & 0 & \alpha_{3,3}(\varepsilon_o) \end{pmatrix}$$

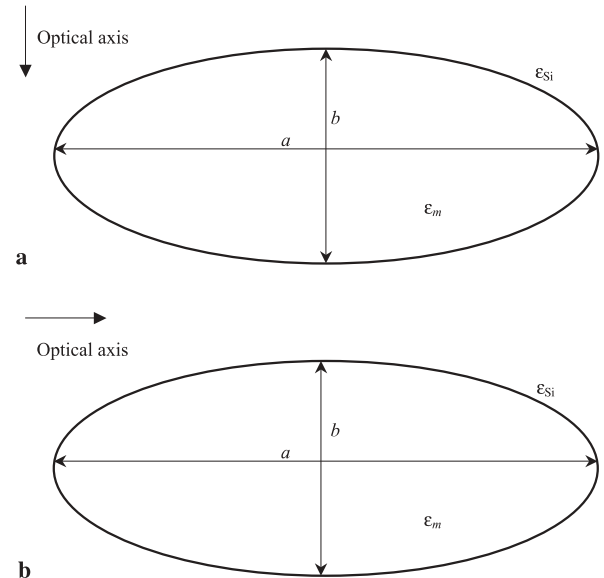


FIGURE 4 (a) Schematic drawing illustrating the orientation of the optical axis of the material consisting of metal-filled porous silicon etched on (110) oriented substrate with respect to the major axis of the metal inclusion ellipsoid for 1st and 2nd inclusion subsets. (b) Schematic drawing illustrating the orientation of the optical axis of the material consisting of metal-filled porous silicon etched on (110) oriented substrate with respect to the major axis of the metal inclusion ellipsoid for 3rd inclusion subsets

where the $\alpha_{i,j}^{(k)}$ coefficients are determined according to (3). We can do so because the optical axis of the effective medium is always aligned with one of the axes of an inclusion ellipsoid for porous silicon etched on (110)-oriented substrate, as illustrated in Fig. 4a for inclusions from 1st and 2nd subsets and Fig. 4b for inclusions from 3rd subset. Silicon “particles” in this approximation can be assumed to have spherical shape. It makes sense to preserve the reference coordinate system in the silicon “particles” matrix. In this case,

$$\hat{\alpha}^{(4)} = \begin{pmatrix} \frac{\varepsilon_{\text{Si}} - \varepsilon_o}{\varepsilon_{\text{Si}} + 2\varepsilon_o} & 0 & 0 \\ 0 & \frac{\varepsilon_{\text{Si}} - \varepsilon_e}{\varepsilon_{\text{Si}} + 2\varepsilon_e} & 0 \\ 0 & 0 & \frac{\varepsilon_{\text{Si}} - \varepsilon_o}{\varepsilon_{\text{Si}} + 2\varepsilon_o} \end{pmatrix}.$$

Hence, (5) can be rewritten into a system of two equations with two unknowns (ε_o and ε_e):

$$\begin{cases} (1-p)\alpha_{1,1}^{(4)} + \frac{p-pr}{4}(\alpha_{1,1}^{(1)} + \alpha_{3,3}^{(1)} + \alpha_{1,1}^{(2)} + \alpha_{3,3}^{(2)}) + pr\alpha_{2,2}^{(3)} = 0 \\ (1-p)\alpha_{2,2}^{(4)} + \frac{p-pr}{2}(\alpha_{2,2}^{(1)} + \alpha_{2,2}^{(2)}) + pr\alpha_{1,1}^{(3)} = 0 \end{cases} \quad (6)$$

Since according to the assumptions the metal “particles” in each of the lattices have the same shape and volume, (6) can be further simplified to:

$$\begin{cases} (1-p)\alpha_{1,1}^{(4)} + \frac{p-pr}{2}(\alpha_{1,1}^{(1)} + \alpha_{3,3}^{(1)}) + pr\alpha_{2,2}^{(3)} = 0 \\ (1-p)\alpha_{2,2}^{(4)} + (p-pr)\alpha_{2,2}^{(1)} + pr\alpha_{1,1}^{(3)} = 0 \end{cases} \quad (7)$$

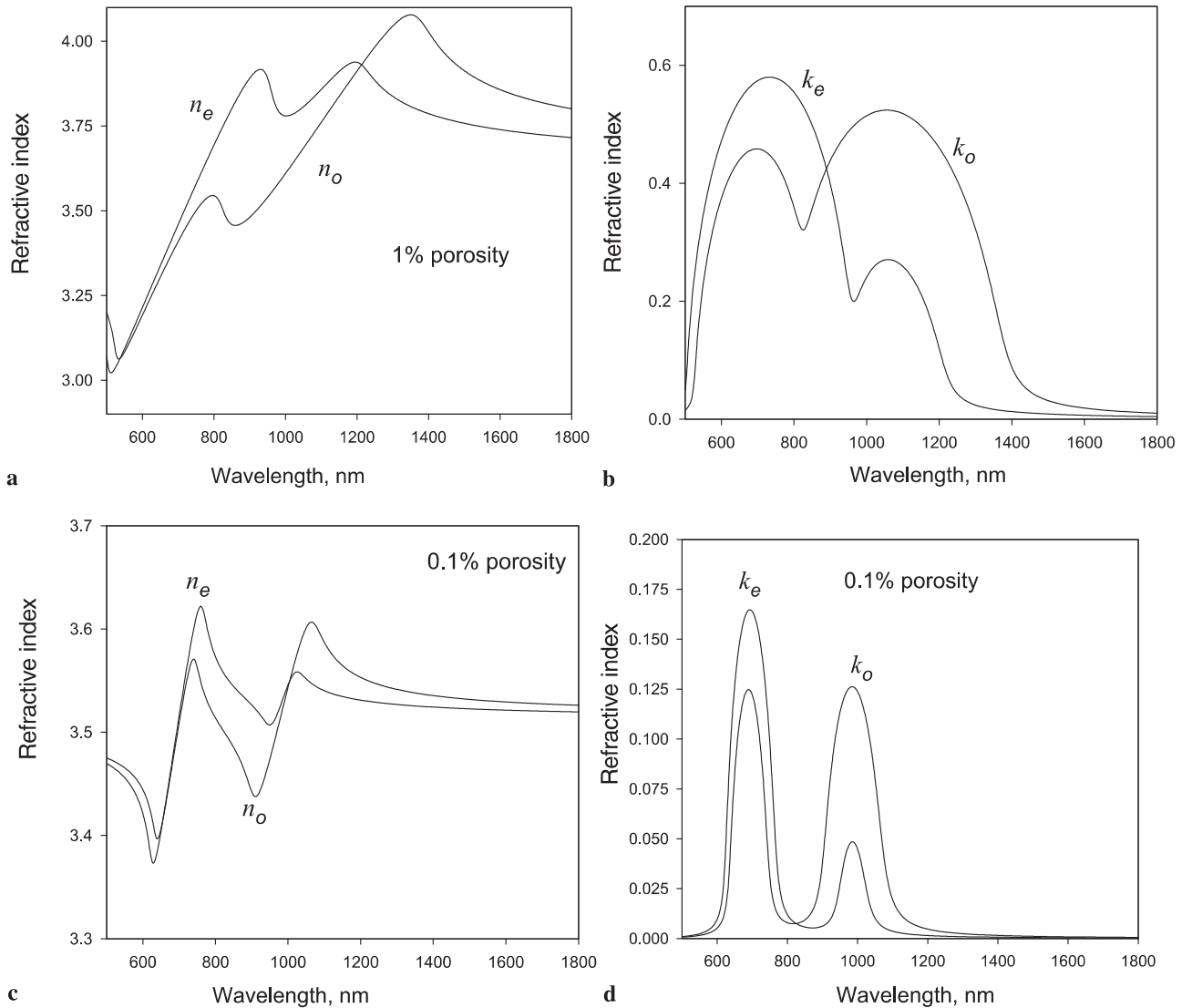


FIGURE 5 (a) Numerically calculated spectral dependences of the real parts of the refractive indices of ordinary and extraordinary waves of the material composed of silver-filled porous silicon etched on (110)-oriented substrate for the case of 1% filling fraction of metal. (b) Numerically calculated spectral dependences of the imaginary parts of the refractive indices of ordinary and extraordinary waves of the material composed of silver-filled porous silicon etched on (110)-oriented substrate for the case of 1% filling fraction of metal. (c) Numerically calculated spectral dependences of the real parts of the refractive indices of ordinary and extraordinary waves of the material composed of silver-filled porous silicon etched on (110)-oriented substrate for the case of 0.1% filling fraction of metal. (d) Numerically calculated spectral dependences of the imaginary parts of the refractive indices of ordinary and extraordinary waves of the material composed of silver-filled porous silicon etched on (110)-oriented substrate for the case of 0.1% filling fraction of metal

Equation (7) can be easily solved numerically.

Based on this model, Fig. 5 gives the numerically calculated spectral dependences of the refractive indices of the ordinary and extraordinary waves for the silver/porous silicon system on (110)-oriented substrate composites. Figures 5a and 5c give the spectral dependences of the real parts of the refractive indices for the composites with 1% and 0.1% metal filling fractions respectively, while Fig. 5b and 5d gives the spectral dependences of the imaginary parts of the refractive indices (also known as attenuation coefficients). In all the figures the silver ellipsoids were assumed to be of an elongated shape with a longer axis of 15 nm and shorter axes of 10 nm. The parameter r (see above) was assumed to be 0.1. One can see that the optical anisotropy of such a material is indeed expected to be quite high. While at 0.1% filling fraction the calculated dependences (Fig. 5c and 5d) of the refractive indices closely resemble those obtained with the generalized Maxwell–Garnet methodology (Fig. 3), for filling fractions still as small as 1%, the spectral dependences are changing shape dramatically. However, the surface plasmon enhancement of the optical anisotropy at certain wavelengths is still very strong.

Figure 6 presents the spectral dependences of the relative optical anisotropies ($|n_o - n_e|/n_o$) of the silver-filled porous silicon etched on (110)-oriented substrate for 0.1% and 1% filling fraction of silver and of the air-filled porous silicon etched on (110)-oriented substrate with 1% porosity. One can see that an almost 100-fold enhancement of the optical anisotropy can be achieved due to the surface plasmon resonance on silver ellipsoids.

The analyzed material can also exhibit quite interesting properties at intermediate filling fractions. For example, Fig. 7 shows the numerically calculated spectral dependences of the dielectric permittivity tensor coefficients for the silver-filled porous silicon etched on (110)-oriented substrate with 17% filling fraction of metal.

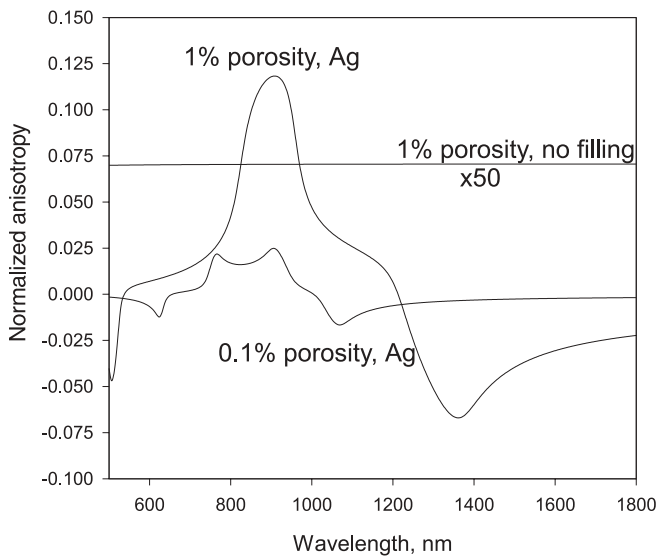


FIGURE 6 Numerically calculated spectral dependences of the relative optical anisotropy of the silver-filled porous silicon etched on (110)-oriented substrate for 0.1% and 1% filling fraction of silver and of the air-filled porous silicon etched on (110)-oriented substrate with 1% porosity (multiplied by 50)

Figure 7a gives the spectral dependences of the real parts of the effective dielectric permittivity tensor coefficients, while Fig. 7b presents the spectral dependences of the imaginary parts of those. One can see that the theory predicts different signs of diagonal elements of effective dielectric permittivity tensor around 1250–1775 nm wavelengths. Materials having these parameters within this spectral range belong to the class of materials with “indefinite” permittivity tensors, using the terminology introduced in [23]. It turns out “indefinite” materials based on porosity offer quite peculiar optical properties. For example, some of the optical modes (surface or bulk) in such materials exist only for certain directions of propagations, but disappear in other directions, a property that can be used in e.g., spatial filter-

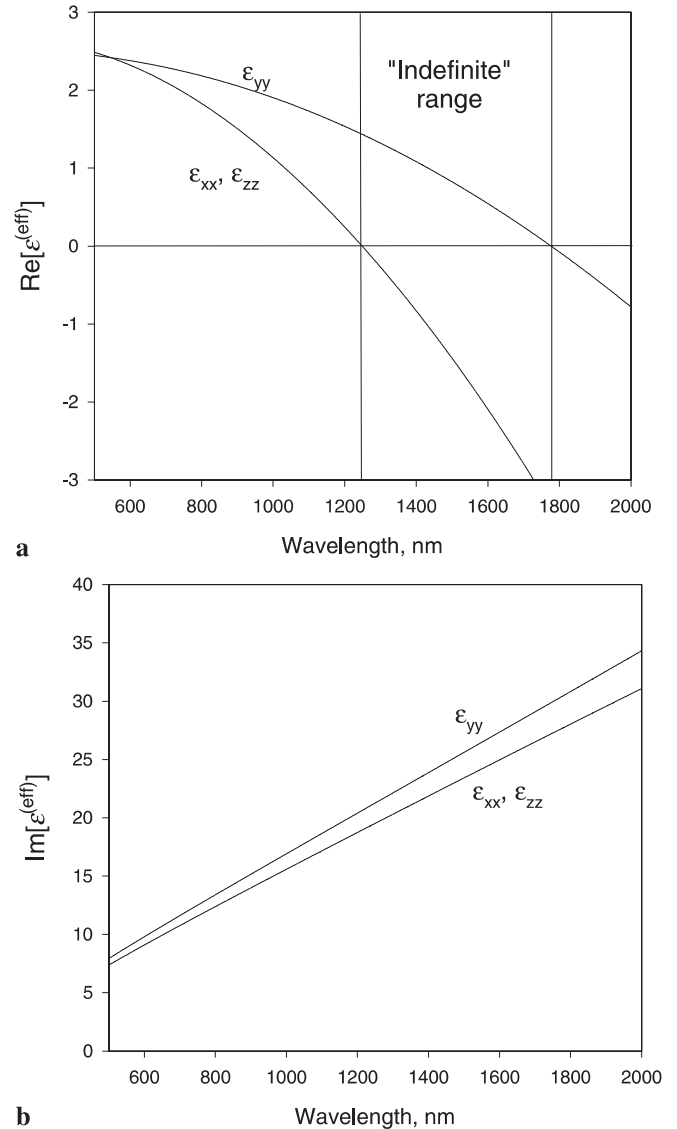


FIGURE 7 (a) Numerically calculated spectral dependences of the real parts of the effective dielectric permittivity tensor coefficients of the material composed of silver-filled porous silicon etched on (110)-oriented substrate for the case of 17% filling fraction of metal (b) Numerically calculated spectral dependences of the imaginary parts of the effective dielectric permittivity tensor coefficients of the material composed of silver-filled porous silicon etched on (110)-oriented substrate for the case of 17% filling fraction of metal

ing. However, it should be noted that according to the model presented here, the losses in the analyzed material within the “indefinite” parameter range will be high (see the large anisotropic imaginary part of the effective dielectric permittivity tensor elements given in Fig. 7b).

Another interesting effect that should take place in the metal-filled porous silicon etched on (110)-oriented substrates is an enhancement of various nonlinear effects, such as Raman scattering and higher order harmonic generation (second, third harmonics, etc.). Such effects should be greatly enhanced due to very high enhancement of the electromagnetic field in the vicinity of metal inclusions. Moreover, uniaxial anisotropy of the analyzed material should make it possible to achieve phase matching (a must in order to get strong coupling between irradiated and double frequency waves). The more detailed consideration of the nonlinear response of analyzed material will be presented in following publications.

3 Conclusions

The generalized Bruggeman effective-medium method for analysis of the dielectric properties of material composed of strongly polarizable metal ellipsoids aligned into several subsets was developed and applied to the case of silver-filled mesoporous silicon etched on (110)-oriented substrate. The uniaxial behavior of such a material was predicted. At small metal filling fractions of the composite material dramatic enhancement of the optical anisotropy was theoretically demonstrated at some wavelengths. It was explained by excitations of the plasmon modes at the surfaces of metal inclusions. It was further predicted that the optical anisotropy of silver-filled mesoporous silicon etched on (110)-oriented substrate would have different signs (positive or negative) at different portions of the spectrum. In addition, it was theoretically demonstrated that such a material might exhibit “indefinite” (meaning different signs of the different elements of the effective dielectric permittivity tensor) dielectric prop-

erties at some wavelengths for intermediate filling fractions. Possible applications of such a material for spatial filtering and nonlinear material were discussed.

REFERENCES

- 1 H. Föll, S. Langa, J. Carstensen, M. Christophersen, I.M. Tiginyanu: *Adv. Materials* **15**, 183 (2003)
- 2 G. Vincent: *Appl. Phys. Lett.* **64**, 2367 (1994)
- 3 V. Pellegrini, A. Tredicucci, C. Mazzoleni, L. Pavesi: *Phys. Rev. B* **52**, 14328 (1995)
- 4 V. Kochergin: *Omnidirectional Optical Filters* (Kluwer Academic Publishers, Boston 2003)
- 5 J. Diener, N. Künzner, D. Kovalev, E. Gross, V.Y. Timoshenko, G. Polisski, F. Koch: *Appl. Phys. Lett.* **78**, 3887 (2001)
- 6 D. Kovalev, G. Polisski, J. Diener, H. Heckler, N. Künzner, V.Y. Timoshenko, F. Koch: *Appl. Phys. Lett.* **78**, 916 (2001)
- 7 J. Diener, N. Künzner, D. Kovalev, E. Gross, F. Koch: *J. Appl. Phys.* **91**, 6704 (2002)
- 8 J. Diener, N. Künzner, E. Gross, D. Kovalev, M. Fujii: *Opt. Lett.* **29**, 195 (2004)
- 9 Q.H. Wu, L. De Silva, M. Arnold, I.J. Hodgkinson, E. Takeuchi: *J. Appl. Phys.* **95**, 402 (2004)
- 10 G. Sauer, G. Brehm, S. Schneider, K. Nielsch, R.B. Wehrspohn, J. Choi, H. Hofmeister, U. Gösele: *J. Appl. Phys.* **91**, 3243 (2002)
- 11 S. Matthias, J. Schilling, K. Nielsch, F. Müller, R.B. Wehrspohn, U. Gösele: *Adv. Mater.* **14**, 1618 (2002)
- 12 H. Kuwata, H. Tamaru, K. Esumi, K. Miyah: *Appl. Phys. Lett.* **83**, 4625 (2003)
- 13 M. Moskovits: *Rev. Mod. Phys.* **57**, 783 (1985)
- 14 D.A.G. Bruggeman: *Ann. Phys. (Paris)* **24**, 636 (1935)
- 15 A.G. Cullis, L.T. Canham, P.D.J. Calcott: *J. Appl. Phys.* **82**, 909 (1997)
- 16 V. Lehmann, R. Stengl, A. Luigart: *Mat. Sci. Eng. B* **69-70**, 11 (2000)
- 17 C. Faivre, D. Bellet: *J. Appl. Cryst.* **32**, 1134 (1999)
- 18 V. Kochergin, M. Christophersen, H. Föll: *Appl. Phys. B*, DOI: 10.1007/s00340-004-1598-z (2004)
- 19 J.C. Maxwell Garnett: *Philos. Trans. R. Soc. London A* **203**, 385 (1904)
- 20 L.D. Landau, E.M. Lifshits: *Electrodynamics of Continuous Media*, 2nd edn. (Butterworth-Heinemann, Oxford 1984)
- 21 *Properties of Porous Silicon*, ed. by L. Canham (IEE Publishing, June 1998)
- 22 A. Yariv, P. Yeh: *Optical Waves in Crystals* (John Wiley & Sons, New York 1984)
- 23 D.R. Smith, D. Schurig: *Phys. Rev. Lett.* **90**, 77405 (2003)